A Detailed Study of the Mass Distribution of the Galaxy Cluster RXC J2248.7-4431

Caminha, G. Bartosch; Rosati, P.; Grillo, Claudio

Published in:
Journal of Physics: Conference Series

DOI:
10.1088/1742-6596/689/1/012005

Publication date:
2016

Document version
Publisher's PDF, also known as Version of record

A Detailed Study of the Mass Distribution of the Galaxy Cluster RXC J2248.7-4431

2016 J. Phys.: Conf. Ser. 689 012005

(http://iopscience.iop.org/1742-6596/689/1/012005)

Journal of Physics: Conference Series **689** (2016) 012005 doi:10.1088/1742-6596/689/1/012005

A Detailed Study of the Mass Distribution of the Galaxy Cluster RXC J2248.7−4431

Gabriel B. Caminha[1], Piero Rosati[1], Claudio Grillo[2] and the CLASH-VLT team

[1]Dipartimento di Fisica e Scienze della Terra, Università degli Studi di Ferrara, Via Saragat 1, I-44122 Ferrara, Italy

[2]Dark Cosmology Centre, Niels Bohr Institute, University of Copenhagen, Juliane Maries Vej 30, DK-2100 Copenhagen, Denmark

E-mail: gbcaminha@fe.infn.it

Abstract. In this work we use strong gravitational lensing techniques to constrain the total mass distribution of the galaxy cluster RXC J2248.7-4432 (RXC J2248, $z_{lens} = 0.348$), also known as Abell S1063, observed within the Cluster Lensing And Supernova survey with Hubble (CLASH). Thanks to its strong lensing efficiency and exceptional data quality from the VIsible Multi-Object Spectrograph (VIMOS) and Multi Unit Spectroscopic Explorer (MUSE) on the Very Large Telescope, we can build a parametric model for the total mass distribution. Using the positions of the multiple images generated by 7 multiply-lensed background sources with measured spectroscopic redshifs, we find that the best-fit parametrisation for the cluster total mass distribution is composed of an elliptical pseudo-isothermal mass distribution with a significant core for the overall cluster halo, and of truncated pseudo-isothermal mass profiles for the cluster galaxies. This model is capable to predict the positions of the multiple images with an unprecedented precision of $\approx 0''.3$. We also show that varying freely the cosmological parameters of the ΛCDM model, our strong lensing model can constrain the underlying geometry of the universe via the angular diameter distances between the lens and the sources and the observer and the sources.

1. Introduction

The concordance ΛCDM cosmological model predicts that, on large scales, the baryonic matter is $\approx 5\%$ of the present energy density of the Universe, and a poorly understood component called dark matter constitutes $\approx 20\%$. A more exotic component, the dark energy Ω_Λ with negative pressure (i.e., with an equation of state of the form $P = w\rho$, where P and ρ are the pressure and the density, respectively, and w is a negative quantity), is responsible for the current accelerated expansion of the Universe [1–3]. On galaxy clusters scales (≈ 1 Mpc) the dominant component is the dark matter, constituting $\approx 90\%$ of the cluster total mass. The rest is composed by hot gas, galaxies and the intra cluster light.

Gravitational lensing effects, i.e. distortion, magnification and creation of multiple images from the same background source, depend on the mass distribution of the midway object acting as a gravitational lens, and on the angular diameter distances between the observer, the lens, and the background source. Note that this effect does not depend on the dynamical state of the lens, making it a powerful probe of the total mass distribution of the lenses and the underlying geometry of the Universe. On galaxy cluster scales, only recently it has been possible

to exploit the observed positions of spectroscopically confirmed families of multiple images to obtain precise measurements of the total mass distributions in the core of these lenses [4, 5] and the first constraint on cosmological parameters [6].

In this work we constrain the total mass distribution of the galaxy cluster RXC J2248 ($z_{lens} = 0.348$) using the images of multiply-lensed background sources. We take advantage of the CLASH multiband *HST* data and extensive spectroscopic information that we have collected on the cluster members and background, lensed sources in this galaxy cluster with the VIMOS and MUSE instruments on the VLT [7, 8].

2. RXC J2248

RXC J2248 was first identified as Abell S1063 in [9] and its high mass and redshift makes it a powerful gravitational lens. It was one of the 25 clusters observed within CLASH [10] in 16 filters, from the UV through the NIR, with the ACS and WFC3 cameras onboard *HST*. These photometric data allow us to identify strong lensing features, such as giant arcs, multiple image families and distorted background sources.

As part of the CLASH-VLT Large program (ID 186.A−0798, P.I.: P. Rosati), the cluster RXC J2248 was observed with the VIMOS spectrograph between June 2013 and May 2015. The inner regions of the galaxy cluster were observed in a total exposure time of 15 hours with 16 masks, 12 with the low-resolution blue grism (spectral resolution of 28Å and wavelength range of $3700 - 6700$Å) and 4 with the intermediate resolution grism (spectral resolution of 13Å and wavelength range $4800 - 10000$Å). Observations with the new integral-field spectrograph MUSE on the VLT were conducted in the South-West part of the cluster as part of the MUSE science verification program (ID 60.A-9345, P.I.: K. Caputi). A 8520 second total exposure was obtained in June 2014 with a seeing of $\approx 1''$. The MUSE data cube covers 1×1 arcmin^2, with a pixel size of $0''.2$, over the wavelength range $4750 - 9350$Å and a dispersion of 1.25 Å. All the details of the VLT and MUSE observations and data reduction can be found in [7] and [8], respectively. From these spectroscopic data, we identified 7 bona-fide spectroscopically confirmed multiple image families. These families do not suffer of systematic effects that we cannot take into account in our parametric model, such as lensing by line of sight mass structures and strong effects of very close cluster members. A discussion of the impact of these effects is given in [11].

3. Strong lensing modelling

We use the strong lensing observables to reconstruct the total mass distribution of RXC J2248. The positions of the multiple images from a single background source depend on the relative distances (observer, lens and source) and on the total mass distribution of the intervening lens. We describe below our methodology to determine the mass distribution of the cluster from the observed positions of the identified multiple images.

3.1. Mass distribution components

In view of its regular shape, we model the total mass distribution of the lens as the sum of three main components: 1) a smooth component describing the extended dark matter, 2) the brightest cluster galaxy (BCG) and 3) small scale halos associated to galaxy members.

For the smooth mass component (intra cluster light, hot gas and, mainly, dark matter) we adopt a Pseudo Isothermal Elliptical Mass Distribution (hereafter PIEMD) [12]. This model has 6 parameters: the centre position (x_0 and y_0), the ellipticity and its orientation angle (ε and θ), the fiducial velocity dispersion (σ_v) and the core radius (r_{core}). The PIEMD parametrization describes well cluster mass distributions in strong lensing studies, and sometimes provides a better fit than the canonical Navarro-Frenk-White (hereafter NFW) [13, 14] mass distribution. In the reference [5], using a similar high-quality data set, it has been found for example that

the dark matter components of the galaxy cluster MACS J0416.1−2403 are better described by PIEMD models.

The galaxy members selection is performed following the method adopted in [5] (see Section 3.3.1 of the referenced paper). Essentially, we investigate the loci of a large sample of spectroscopically confirmed cluster members and field galaxies in a multidimensional color space. We then model the probability density distributions (PDFs) of cluster member and field galaxy colours as multidimensional gaussians, with means and covariances determined using the Minimum Covariance Determinant [15]. We label each galaxy as being a cluster member or a field galaxy, using the determined PDFs in a Bayesian hypotheses inference. We then classify galaxies using a probability threshold that is a good compromise between purity and completeness, and thus selecting additional cluster members with no spectroscopic redshifts. With this procedure we select a total of 139 cluster members in the model within a distance of $1'$ from the BCG, 64 of which are spectroscopically confirmed. Each cluster member is modelled as a truncated PIEMD [16,17] with zero ellipticity and core radius, and a finite truncation radius. Following a standard procedure in cluster-scale strong lensing analyses, we reduce the number of free parameters describing the cluster members assuming a constant total mass-to-light ratio of cluster members. Thus, we are left with only two parameters, the reference velocity dispersion σ_v^{gals} and truncation radius r_{trunc}^{gals}, describing the overall properties of all cluster members.

Due to a generally different formation history, the BCG is often observed to significantly deviate from this scaling relation [18]. We therefore introduce two additional free parameters associated to the BCG (σ_v^{BCG} and r_{trunc}^{BCG}), keeping its position fixed at the center of the light distribution. We eventually have a total of 10 free parameters to describe the total mass distribution of RXC J2248.

3.2. Lensing modelling definitions

The strong lensing modelling is performed using the public software *lenstool* [19, 20]. Once the model components are defined, the best-fit model parameters are found by minimizing the distance between the observed and predicted positions of the multiple images, and the parameter covariance is quantified using a Bayesian Markov Chain Monte Carlo (MCMC) technique. In detail, to find the best-fitting model, we define the lens plane χ^2 function as follows:

$$\chi^2(\vec{\Pi}) := \sum_{j=1}^{N_{\rm fam}} \sum_{i=1}^{N_{\rm im}^j} \left(\frac{\left| \vec{\theta}_{i,j}^{\rm obs} - \vec{\theta}_{i,j}^{\rm pred}\left(\vec{\Pi}\right) \right|}{\sigma_{i,j}^{\rm obs}} \right)^2 , \tag{1}$$

where $N_{\rm fam}$ and $N_{\rm im}^j$ are the number of families and the number of multiple images belonging to the family j, respectively. $\vec{\theta}^{\rm obs}$ and $\vec{\theta}^{\rm pred}$ are the observed and the predicted positions of the multiple images, and $\sigma^{\rm obs}$ is the uncertainty in the observed position. The predicted position of an image is a function of both lens parameters and cosmological parameters, all represented by the vector $\vec{\Pi}$. In this work we adopt flat priors on all parameters. The set of parameters $\vec{\Pi}$ that provides the minimum value of the χ^2 function (χ^2_{min}) is called the best-fitting model, while the predicted positions of this model are referred to as $\vec{\theta}^{\rm bf}$.

3.3. The family ratio

The availability of a large number of multiple images with measured spectroscopic redshifts and a relatively regular mass distribution, makes RXC J2248 a suitable cluster lens to test the ability to constrain cosmological parameters. Strong lensing is sensitive to the underlying geometry of the Universe via the angular diameter distances between the observer and the lens (D_{OL}), the observer and the source (D_{OS}), and the lens and the source (D_{LS}). For one source, the lens

equation can be written as

$$\vec{\theta} = \vec{\beta} + \frac{D_{LS}}{D_{OS}} \hat{\vec{\alpha}} \left(\vec{\theta} \right), \tag{2}$$

where $\vec{\theta}$ and $\vec{\beta}$ are the angular positions on the lens and source planes, respectively, $\hat{\vec{\alpha}}$ is the deflection angle and the cosmological dependence is embedded into the angular diameter distances. The ratio between the cosmological distances is degenerated with the parameters of the lens mass distribution. However, when a significant number of multiply lensed sources at different redshifts is present, this degeneracy can be broken and a leverage on cosmological parameters can be obtained via the so called family ratios:

$$f_k(\vec{\pi}) = \frac{D(\vec{\pi})_{LS,1} D(\vec{\pi})_{OS,2}}{D(\vec{\pi})_{LS,2} D(\vec{\pi})_{OS,1}}, \tag{3}$$

where $\vec{\pi}$ is the set of cosmological parameters and 1 and 2 are two different sources at redshifts z_{s1} and z_{s2}.

This technique has been successfully applied to the galaxy clusters Abell 2218 [21] and Abell 1689 [6]. In this work, we use the ΛCDM cosmological model, which includes as free parameters the energy density of the total matter of the universe (ordinary and dark matter) Ω_m, the dark energy density Ω_Λ and the equation of state parameter of this last component, $w = P/\rho$. All results from our lens model are summarized in the next Sections.

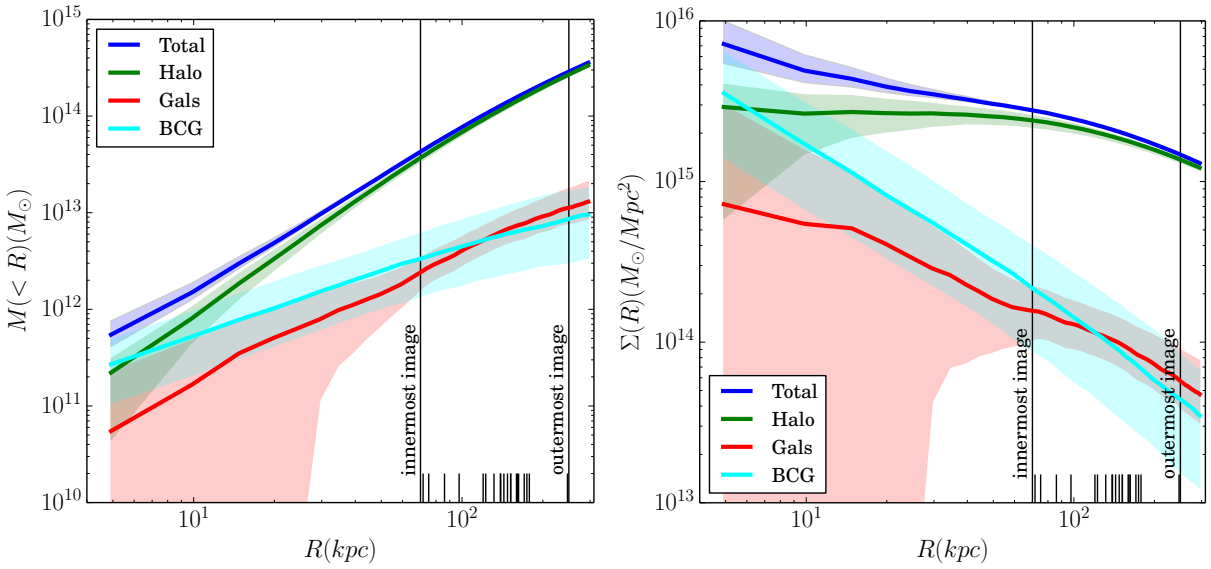

Figure 1. Projected mass, $M(< R)$, and surface mass density $\Sigma(R)$ relatively to the BCG center for the total, cluster dark-matter (Halo), galaxy members (Gals) and BCG mass components. The solid lines represent the median and the filled contours the 68% confidence level from the strong lensing total mass reconstruction. The vertical lines show the positions of the multiple images.

4. Results

We first consider a model fixing the cosmological parameters to $\Omega_m = 0.3$, $\Omega_\Lambda = 0.7$ and $w = -1$, i.e., a flat cosmology with a cosmological constant. We use this model to study

the overall properties of the cluster total mass distribution. Secondly, we let the cosmological parameter free, together with those parametrizing the total mass distribution. In this case, we consider a flat ΛCDM model (i.e. $\Omega_\Lambda = 1 - \Omega_m$), and varying Ω_m and w. The parameters of this model are constrained via the family ratios (see Equation 3). In both cases, the mean offset between the observed and predicted positions of the images is $\approx 0''.3$, showing that our models can reproduce the observations with high accuracy.

4.1. Constraining the mass distribution

In the left panel of Figure 1, we show the reconstructed projected mass as a function of the radius, considering the BCG centre as reference, using our strong lensing model with fixed cosmological parameters. The solid lines are the medians and the filled regions are the 68% confidence levels for different mass components: total, dark-matter (Halo), galaxy members (Gals) and BCG. The vertical black lines indicate the distance of the multiple images to the BCG center. The larger statistical uncertainties on the recovered mass components, especially for the BCG and the galaxy members, in the innermost regions of the cluster (i.e. $R < 30\,\mathrm{kpc}$) are a consequence of the lack of multiple images in these regions. However, these uncertainties decrease significantly in the outskirts, $R > 50\,\mathrm{kpc}$, as expected due to the presence of the multiple image constraints. We find that, the total projected mass within 250 kpc is $2.90^{+0.03}_{-0.03} \times 10^{14} M_\odot$ (the errors are given by the 68% confidence level) in our model, higher than the values of $2.68^{+0.03}_{-0.05} \times 10^{14} M_\odot$ and $2.67^{+0.08}_{-0.08} \times 10^{14} M_\odot$ presented in [22] and [23], respectively. Although these measurements are not consistent within the statistical errors, the mean values do not differ by more than 10%, and are likely due to different assumptions in these studies. We show the surface mass density given by our model in the right panel of Figure 1. It is interesting to note that the dark matter halo component, green line and filled regions, shows a relatively flat density up to $R \approx 100\,\mathrm{kpc}$.

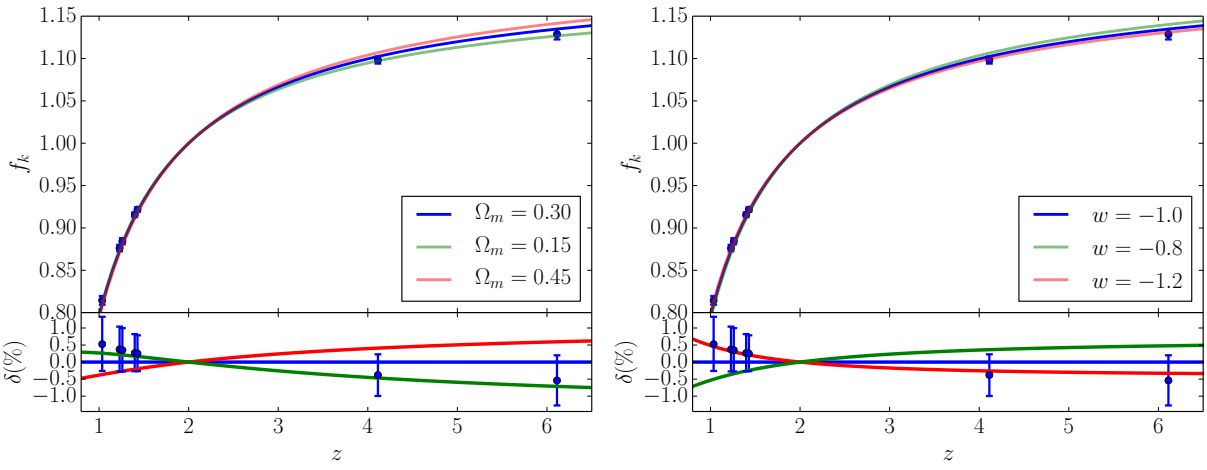

Figure 2. Top panels: family ratios f_k of our strong lensing modelling with free cosmology as a function of redshift, renormalized for $z_{s2} = 2$. The blue circles show the best fit values from the lens model and the error bars are the 68% confidence level. The continuous lines show the the family ratios with fixed values of the cosmological parameters. Bottom panels: relative difference with respect to the concordance flat ΛCDM model (i.e. $\Omega_m = 0.3$ and $w = -1$).

4.2. Recovering the family ratios f_k

In Figure 2, we show the family ratios of the observed sources renormalized for a source at $z_{s2} = 2$ (see Equation 3), from our best-fitting strong lensing model with free cosmological parameters. In the top panels, the blue circles and the error bars are the median and the 68% confidence level and the continuous lines the prediction of the ΛCDM model with different values of Ω_m (left panel) and w (right panel). In the bottom panels we show the relative difference δ with respect to the concordance flat ΛCDM model (i.e. $\Omega_m = 0.3$ and $w = -1$). The statistical scatter given by the error bars is a result of degeneracies between f_k and the mass distribution parameters. Our modelling seems to favour models with lower values of w and Ω_m when comparing with the concordance model, however the error bars do not exclude this cosmological model. Moreover, the wide range of the source redshifts, from 1.0 to 6.1 is critical to yield good constraints on the evolution of f_k up to high values of z. A complete study of the cosmological constraints using the galaxy cluster RXC J2248 is presented in [11].

5. Conclusions

Using the positions of spectroscopically confirmed multiply lensed images, we obtain a detailed reconstruction of the total mass distribution of the galaxy cluster RXC J2248. Although the scatter is larger for the mass components of the galaxy members and the BCG in the innermost regions, $R < 30$kpc, in the outer regions these components are well constrained. We show that RXC J2248 is particularly suitable for constraining the background geometry of the Universe with strong lensing modelling due to its unique combination of a regular shape and a large number of multiple images spanning a wide redshift range, as revealed by our spectroscopic survey.

References

[1] Riess A G *et al.* 1998 *AJ* **116** 1009
[2] Eisenstein D J *et al.* 2005 *ApJ* **633** 560
[3] Planck Collaboration 2014 *A&A* **571** A16
[4] Halkola A *et al.* 2008 *A&A* **481** 65–77
[5] Grillo C *et al.* 2015 *ApJ* **800** 38
[6] Jullo E *et al.* 2010 *Science* **329** 924
[7] Balestra I *et al.* 2013 *A&A* **559** L9
[8] Karman W *et al.* 2015 *A&A* **574** A11
[9] Abell G O *et al.* 1989 *ApJS* **70** 1
[10] Postman M *et al.* 2012 *ApJS* **199** 25
[11] Caminha G B *et al.* 2015 *ArXiv:1512.04555*
[12] Kassiola A and Kovner I 1993 *ApJ* **417** 450
[13] Navarro J F *et al.* 1996 *ApJ* **462** 563
[14] Navarro J F 1997 *ApJ* **490** 493–508
[15] Rousseeuw P J 1984 *JASA* **79** 871
[16] Elíasdóttir A *et al.* 2007 *ArXiv:0710.5636*
[17] Suyu S H and Halkola A 2010 *A&A* **524** A94
[18] Postman M *et al.* 2012 *ApJ* **756** 159
[19] Kneib J P *et al.* 1996 *ApJ* **471** 643
[20] Jullo E *et al.* 2007 *New Journal of Physics* **9** 447
[21] Soucail G *et al.* 2004 *A&A* **417** L33
[22] Johnson T L *et al.* 2014 *ApJ* **797** 48
[23] Monna A *et al.* 2014 *MNRAS* **438** 1417